Fluoride Inhibition of *Klebsiella aerogenes* Urease: Mechanistic Implications of a Pseudo-uncompetitive, Slow-Binding Inhibitor†

Matthew J. Todd‡ and Robert P. Hausinger*

Departments of Biochemistry and Microbiology, Michigan State University, East Lansing, Michigan 48824

Received October 4, 1999; Revised Manuscript Received March 6, 2000

ABSTRACT: *Klebsiella aerogenes* urease uses a dinuclear nickel active site to catalyze the hydrolysis of urea. Here, we describe the steady-state and pre-steady-state kinetics of urease inhibition by fluoride. Urease is slowly inhibited by fluoride in both the presence and absence of substrate. Steady-state rate studies yield parallel double-reciprocal plots; however, we show that fluoride interaction with urease is not compatible with classical uncompetitive inhibition. Rather, we propose that fluoride binds to an enzyme state (E*) that is in equilibrium with resting enzyme (E) and produced during catalysis. Fluoride binding rates are directly proportional to inhibitor concentration. Substrate reduces both the rate of fluoride binding to urease and the rate of fluoride dissociation from the complex, consistent with urea binding to E* and E*·F in addition to E. Fluoride inhibition is pH-dependent due to a protonation event linked to fluoride dissociation. Fluoride binding is pH-independent, suggesting that fluoride anion, not HF, is the actual inhibitor. We assess the kinetic results in terms of the known protein crystal structure and evaluate possible molecular interpretations for the structure of the E* state, the site of fluoride binding, and the factors associated with fluoride release. Finally, we note that the apparent uncompetitive inhibition by fluoride as reported for several other metalloenzymes may need to be reinterpreted in terms of fluoride interaction with the corresponding E* states.

Urease (urea amidohydrolase, E.C. 3.5.1.5) catalyzes the hydrolysis of urea to form ammonia and carbamate (*1*). The latter product spontaneously decomposes to yield a second molecule of ammonia and carbon dioxide. High concentrations of ammonia arising from these reactions, as well as the accompanying pH elevation, have important implications in medicine and agriculture. For example, urease serves as a virulence factor in pathogens that are responsible for the development of kidney stones, pyelonephritis, peptic ulcers, and other medical complications (reviewed in ref *2*). Furthermore, soil-derived urease activity rapidly degrades urea-based fertilizers—contributing to phytopathic effects and loss of volatilized nitrogen (*3*). The enzyme also plays a critical role in the nitrogen metabolism of many microorganisms and plants (*2*, *4*). Even before the medical and agricultural importance of urease was appreciated, the enzyme had a rich history. In 1926, the protein from jack bean seeds was the first enzyme to be crystallized (*5*). Nearly 50 years later, this plant protein was the first enzyme demonstrated to possess nickel (*6*). Although interest in the plant enzyme has continued, most recent urease-related studies have focused on analysis of the bacterial genes and enzymes (*2*).

The structure and mechanism of urease is best characterized for the enzymes derived from *Klebsiella aerogenes* (reviewed in ref *1*) and *Bacillus pasteurii* (*7*). Crystallographic analyses of the *K. aerogenes* enzyme first revealed the dinuclear nickel active site with the two metals (separated by 3.6 Å) being bridged by a carbamylated lysine and a hydroxide (WB) (*8*, *9*). The five-coordinate Ni-1 also possesses two histidyl ligands and a terminally coordinated water molecule (W1). Ni-2 is six-coordinate, including two histidyl groups, one aspartyl group, and a terminally coordinated water (W2) ligand. An analogous active-site structure is present in *B. pasteurii* urease (*7*). Comparison of the two structures shows that a protein flap covers the active site in the *K. aerogenes* protein but is extended into solution in the *B. pasteurii* urease structure. This lid is suggested to move during the catalytic cycle, with an open structure being needed for substrate entry or product release while a closed flap is required for catalysis. Two distinct structurally based mechanisms have been proposed for urease (Figure 1). These mechanisms (*1*, *7*) differ in the binding mode for urea, the identity of the attacking hydroxide, and the role of the nearby catalytic histidine group (His 320 in the *K. aerogenes* numbering). Current efforts are focused on testing these mechanistic hypotheses, including the analysis of urease inhibitors.

Fluoride ion was first demonstrated to inhibit bovine rumen urease in 1943 (*10*), yet the detailed mechanism of inhibition remains unclear. Several groups have described the inhibition of jack bean urease by fluoride as being competitive (*11*−*13*). Fluoride binding also was shown to be mutually exclusive with binding of known competitive inhibitors (e.g., β-mercaptoethanol; *12*). That same study reported, however, that fluoride inhibition was time-dependent and yielded

† This work was supported by USDA Grant 9803562 and its predecessors.

* To whom correspondence should be addressed at 160 Giltner Hall; Phone 517-353-9675; Fax 517-353-8957; E-mail Hausinge@pilot.msu.edu.

‡ Present address: Department of Biology, The Johns Hopkins University, Baltimore, MD 21218.

10.1021/bi992287m CCC: $19.00
Published on Web 04/13/2000

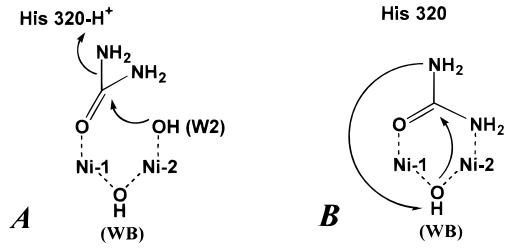

FIGURE 1: Alternative mechanisms proposed for urease. (A) The mechanistic proposal developed from studies of *K. aerogenes* urease suggests that urea displaces W1 from the resting state of the enzyme and coordinates via its carbonyl oxygen to Ni-1. The hydroxide form of W2 ($pK_a \sim 9$ for protonation to water) attacks the urea carbonyl, forming a tetrahedral intermediate. Protonated His 320 ($pK_a \sim 6.5$) donates a proton to one urea amine that is released as ammonia, and carbamate dissociates into solution where it spontaneously decomposes. Because the group with a higher pK_a must be deprotonated while the group with the lower pK_a must be protonated, this is termed the "reverse-protonation" mechanism (*1*). (B) An alternative mechanism developed from studies of the *B. pasteurii* enzyme suggests that the urea carbonyl binds to Ni-1 and one of its amine groups binds to Ni-2. WB in its hydroxy state ($pK_a \sim 9$ for deprotonation to the oxydianion) attacks the carbonyl as it donates a proton to the second amine (stabilized by deprotonated His 320). Finally, carbamate and ammonia products are released (*7*).

steady-state values that were consistent with uncompetitive inhibition. The authors proposed that a ternary enzyme−urea−fluoride complex was formed. The discrepancies in the reported mechanism of fluoride inhibition, coupled with the fact that uncompetitive inhibition is rarely reported for single-substrate enzymes (e.g., *14*−*19*), stimulated our efforts to characterize the action of this inhibitor on *K. aerogenes* urease.

We demonstrate that fluoride is a pseudo-uncompetitive, slow-binding inhibitor of *K. aerogenes* urease. We propose a novel mechanism for inhibition in which fluoride anion binds to a form of the enzyme (E*) that is in equilibrium with the resting state (E) and transiently generated during catalysis. Furthermore, we suggest that substrate binds to E, E*, and the E*·F complex. We show that the effects of fluoride, urea, and pH on the rates of fluoride binding and dissociation are consistent with the proposed model. On the basis of the known urease crystal structures, we evaluate possible molecular models to account for E*, the site of fluoride binding, and the pH dependence of fluoride dissociation. Finally, we suggest that a model involving E and E* states may have wider applicability to explain the apparent uncompetitive inhibition results for other metalloenzymes.

EXPERIMENTAL PROCEDURES

Urease Purification and Assay. *K. aerogenes* urease was purified as previously described (*20*) from recombinant *K. aerogenes* CG253 (pKAU19) cells (*21*), after growth in MOPS medium supplemented with 1 mM $NiCl_2$. These cells contained two copies of the *K. aerogenes* urease gene cluster: the original genomic copy and an IPTG-inducible plasmid-borne copy. The purified enzyme possessed a specific activity of 2500 μmol·min^{-1}·(mg of protein)$^{-1}$ when assayed under standard conditions: 37 °C in 50 mM HEPES buffer (pH 7.75) containing 1 mM EDTA and 50 mM urea. The released ammonia was measured after its conversion to indophenol (*22*). One unit of urease activity is defined as the ability to degrade 1 μmol of urea min^{-1}. Protein concentrations were determined according to Lowry et al. (*23*) with bovine serum albumin as the standard.

Inhibitor Binding and Dissociation Rates. Nonlinear progress curves (plots of product accumulation with time, $P_{(t)}$] were fit to an exponential decay function (eq 1) by using KaleidaGraph software to obtain the initial rate of urea hydrolysis (v_i), the final steady-state rate (v_f), and the observed binding (or dissociation) rate, k_{obs}:

$$P_{(t)} = P_{(0)} + v_f t + (v_i - v_f)(1 - \exp^{-k_{obs}t}) \qquad (1)$$

Alternatively, k_{obs} for inhibitor binding was derived from the slopes of plots that compared the natural logarithms of the instantaneous rates versus time.

Dissociation rates of fluoride-inhibited urease were measured by diluting (>100-fold) preformed inhibited complex into buffer plus various concentrations of substrate. Inhibited complex was formed by incubating urease with 1 mM fluoride and 1 mM urea for 1 min at pH 6, where steady-state fluoride inhibition studies showed a $K_d \sim 10$ μM (see Results).

Fluoride inhibition of urease was unrelated to trace contamination by aluminum ion giving rise to the well-known inhibitory effects of aluminofluoride on many enzymes (*24*). Added Al^{3+} had no effect on the steady-state K_i or on the rate of inhibition. Similarly, the presence of added ammonia affected neither the inhibition constant nor the rate of inhibition. Finally, control experiments demonstrated that fluoride had no effect on the reaction of ammonia to form indophenol during the assay.

RESULTS

Slow-Binding Urease Inhibition by Fluoride. Progress curves showing the amount of product formed over time for *K. aerogenes* urease in the presence and absence of fluoride are shown in Figure 2. The rates of urea hydrolysis in the absence of fluoride (traces A and B) were constant during the time course of these experiments. In the presence of fluoride (traces C−G), however, the rate decreased from that observed initially (v_i) to reach new, steady-state values (v_f). Fluoride concentration had a significant effect on the observed inhibitor binding rates (k_{obs}) (e.g., the onset of inhibition was more rapid at greater inhibitor concentrations) and on the steady-state level of inhibition (v_f) (compare trace C to trace E and trace D to trace F in Figure 2). All data were fit to eq 1 (see Experimental Procedures) to obtain estimates for v_i, v_f, and k_{obs} (Table 1).

Order-of-addition experiments showed that reactions initiated by adding enzyme to mixtures of urea plus fluoride had values of v_i that were indistinguishable from rates observed in the absence of fluoride (Figure 2, traces A, C, and E). In contrast, incubating urease with fluoride for 5 min (traces D and F) or 60 min (trace G) prior to addition of substrate led to decreases in v_i followed by further decreases in rate. For any particular concentration of fluoride, the values of k_{obs} and v_f were statistically identical whether enzyme was first incubated with fluoride (Table 1). Further experiments were designed to assess the effects of fluoride concentration, urea concentration, and pH on each of these kinetic parameters.

Steady-State Rate Analysis of Fluoride Inhibition. Analyses of steady-state reaction rates (i.e., values of v_f) as functions

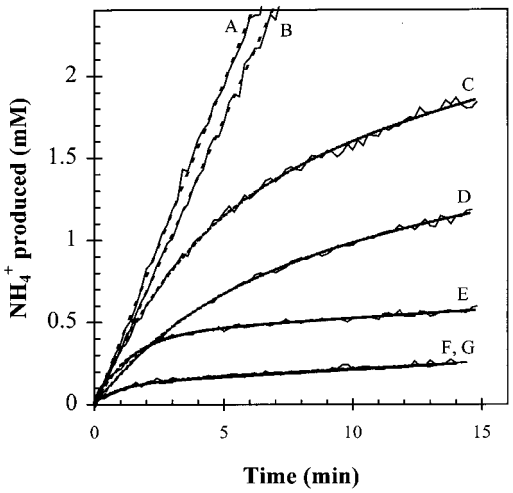

FIGURE 2: Slow-binding inhibition of K. aerogenes urease by fluoride. Urease (final concentration of 0.72 nM) was incubated for 0 min (trace A) or 60 min (trace B) at 37 °C in standard assay buffer (50 mM HEPES, pH 7.75, and 1 mM EDTA) prior to addition of urea (25 mM final concentration), leading to linear increases in product formation (assayed every 0.2 min). Linear regression analyses yielded the rates shown in Table 1. Inclusion of 2.5 mM NaF (traces C and D) or 10 mM NaF (traces E−G) led to progressive decreases in the observed rates of urease activity. Samples were incubated with fluoride for 0 min (traces C and E), 5 min (traces D and F), or 60 min (trace G) prior to addition of substrate. Raw data are plotted as thin lines; the dashed, thick lines represent the best fit to eq 1 with values of v_i, k_{obs}, and v_f as provided in Table 1.

Table 1: Kinetic Analysis of Fluoride Binding to Urease[a]

trace	[fluoride] (mM)	incubation time (min)	v_i (μM·min^{-1})	k_{obs} (min^{-1})	v_f (μM·min^{-1})
A	0	0	0.38 ± 0.01		
B	0	60	0.35 ± 0.01		
C	2.5	0	0.38 ± 0.01	0.26 ± 0.02	0.039 ± 0.005
D	2.5	5	0.20 ± 0.01	0.22 ± 0.02	0.027 ± 0.004
E	10	0	0.31 ± 0.02	0.73 ± 0.03	0.010 ± 0.001
F	10	5	0.11 ± 0.01	0.78 ± 0.09	0.008 ± 0.001
G	10	60	0.012	0.98 ± 0.13	0.009 ± 0.001

[a] Raw data were obtained from Figure 2 under conditions described in the figure legend and under Experimental Procedures. Data were fit to eq 1.

of urea and fluoride ion concentrations were consistent with uncompetitive inhibition; i.e., fluoride led to decreased values of V_{max}, increased values of K_m, and a series of parallel lines in double-reciprocal plots (Figure 3A). When these analyses were extended over a range of pH values, fluoride inhibition continued to appear uncompetitive (data not shown), but the apparent K_i exhibited a dramatic pH dependence (Figure 3B). A plot of log (K_i) versus pH (Figure 3B) yielded a slope of 1, linking fluoride inhibition to a protonation event.

Rate of Fluoride Binding to Urease. Progress curves such as those shown in Figure 2 were generated for a variety of inhibitor/substrate concentrations. Values of k_{obs} (derived from fits to eq 1) were found to be directly proportional to inhibitor concentration (Figure 4A), as expected for a second-order reaction. The observed rate constants were divided by the fluoride concentrations to provide apparent second-order binding constants (k_{app}). Figure 4A reveals that substrate concentration had a pronounced effect on k_{app}, and in Figure 4B this effect is illustrated more clearly by comparing k_{app} as a function of urea concentration. With increasing substrate

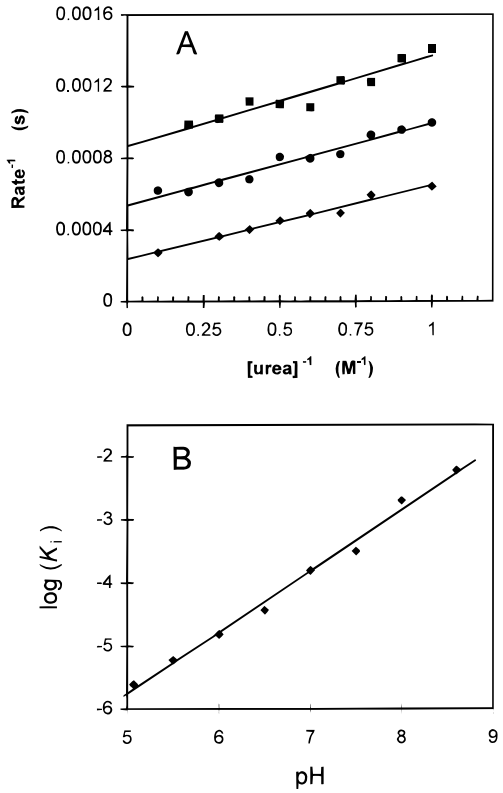

FIGURE 3: Pseudo-uncompetitive steady-state inhibition by fluoride. (A) Steady-state rates for urea hydrolysis were obtained at the indicated concentrations of urea by measuring the amount of ammonia produced after 20, 40, 60, and 80 min of reaction in 100 mM HEPES and 5 mM EDTA, pH 7.0 (37 °C) plus 0 (◆), 100 (●), or 200 μM (■) NaF. Assays were designed so that substrate depletion was insignificant in all cases. (B) Inhibition constants were determined at the indicated pH values in 100 mM HEPES (pH 6.5−8.6) or 100 mM MES (pH 5−7), plus 5 mM EDTA, and varying concentrations of urea and fluoride. Steady-state inhibition constants were determined by standard formulas. Linear regression analysis of the data yielded a line ($r = 0.992$) with slope = 0.97 ± 0.035.

concentration, k_{app} decreased. These data suggest that urea inhibits fluoride binding. The data in Figure 4B were fit to a standard hyperbolic equation to determine the maximum k_{app} (7.7 M^{-1} s^{-1}) and the K_s for urea inhibition of fluoride binding (12.5 mM).

Dissociation of the Urease−Fluoride Complex. The reactivation of fluoride−urease complex was also a slow process, occurring over several minutes. Fluoride-inhibited urease was generated in the presence of substrate at low pH, where the K_d for fluoride dissociation is ~10 μM (Figure 3B). Following a large dilution, dissociation was measured in the absence or presence of substrate (Figure 5, panels A and B, respectively). When the fluoride-inhibited urease complex was diluted into buffer that lacked substrate (Figure 5A), aliquots were shown to increase in specific activity and approached the value observed for uninhibited enzyme [2500 units·(mg of protein)$^{-1}$]. Data yielded a first-order dissociation constant (k_{off}) of 0.0133 s^{-1}. Alternatively, when the inhibited complex was diluted into buffer containing substrate, reactivation of inhibited enzyme was much slower (Figure 5B). Data were fit to eq 1 with $v_i = 0$ to obtain apparent first-order dissociation constants. These values of k_{obs} are plotted vs substrate concentration in Figure 5C and were fit to a standard hyperbolic equation to yield K_s of 1.8

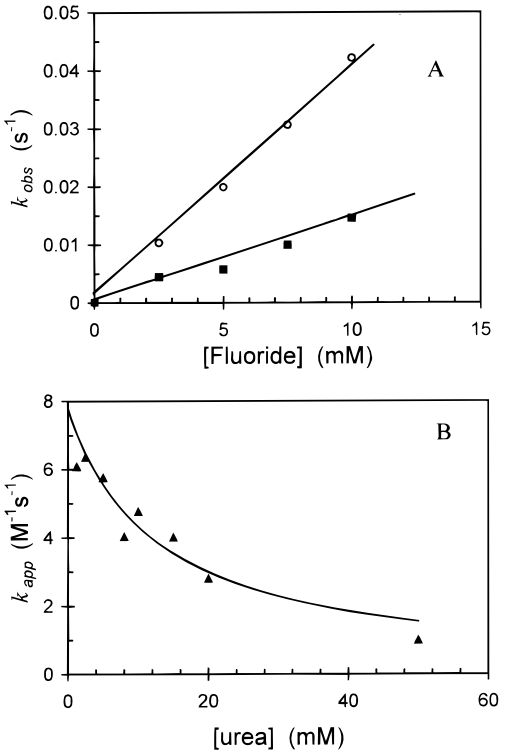

FIGURE 4: Apparent second-order rate constants for fluoride binding. (A) Observed rates of fluoride binding (k_{obs}) were measured as described in Figure 2 for samples containing 2.5 mM urea (○) or 50 mM urea (■) in the presence of the indicated concentrations of fluoride. Regression of the data gave apparent second-order rates (k_{app}) for fluoride binding. (B) Analogous values of k_{app} were collected for the indicated concentrations of urea. Data (average of 3−5 determinations) were fit to the hyperbolic equation $k_{app} = k_{app(max)}\{K_{s,urea}/(K_{s,urea} + [urea])\}$ to give the second-order rate constant, $k_{app(max)} = 7.7\ M^{-1}\ s^{-1}$ and $K_{s,urea} = 12.5$ mM.

mM for substrate inhibition of the reactivation of urease−fluoride complex.

Effect of pH on Binding and Dissociation Rates. An equilibrium K_i can be expressed as the ratio of the microscopic binding and dissociation rates (*25*). Given the marked effect of pH on the equilibrium values of K_i (Figure 3B), one of these two microscopic rate constants must also be pH-dependent. The apparent binding rate, k_{app} (e.g., Figure 4B), was determined as a function of pH and is plotted in Figure 6 (▲). This rate was nearly pH-independent, increasing ~3-fold as the pH decreased from 9 to 6. The dissociation rate was also examined as a function of pH, both in the absence of urea (yielding k_{off} as in Figure 5A) and in the presence of urea (giving k_{obs} as in Figure 5B). In the absence of urea, the reactivation rate decreased ~5-fold from pH 9 to 6 (Figure 6, ○). In the presence of urea, however, a much larger pH dependence on the reactivation rate was observed: k_{obs} changed several orders of magnitude over this pH range (Figure 6, □).

DISCUSSION

Steady-State Kinetic Analysis of Urease Inhibition by Fluoride. The set of parallel lines seen in the double-reciprocal plot of Figure 3A suggests either of two interpretations. (1) Classical uncompetitive inhibition (Scheme 1), as described in many kinetics texts (*25*), occurs when an inhibitor binds to an enzyme−substrate complex. This type

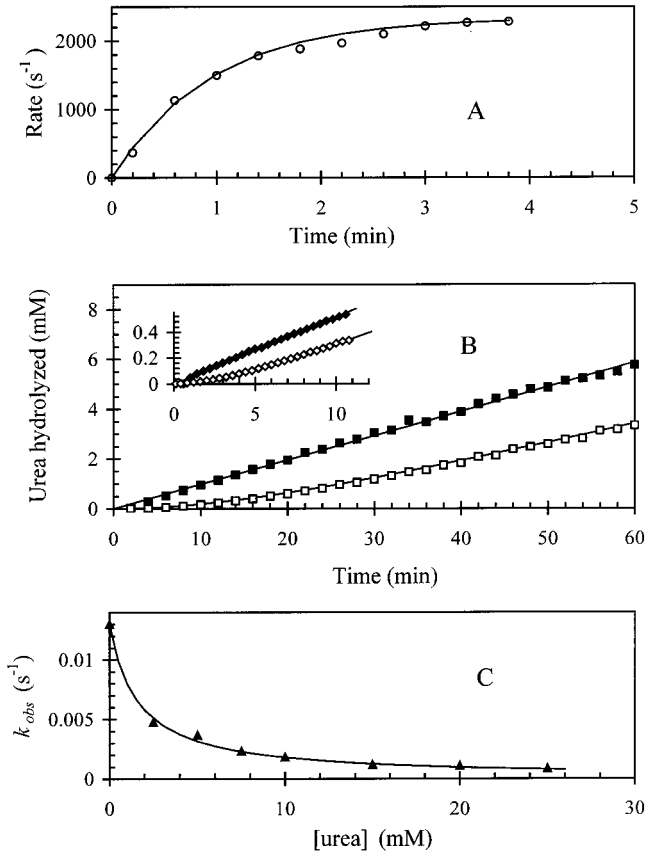

FIGURE 5: First-order fluoride dissociation rate constants. (A) Dissociation of the fluoride−urease complex in the absence of urea was measured by diluting preformed complex 200-fold into buffer lacking urea, then adding substrate (to 100 mM) at the indicated times, and determining activity over 1 min. During this time, little additional complex dissociated (since high substrate concentration inhibits the dissociation rate—e.g., panel B). (B) Dissociation of the fluoride−urease complex in the presence of urea was measured by dilution (>100 fold) into 50 mM urea in standard assay buffer (open symbols). A second sample, treated similarly but in the absence of fluoride, was also assayed as a control (closed symbols). Activity in the control was linear, whereas preformed enzyme−fluoride complex increased in activity over time. Data were fit to eq 1 with $v_i = 0$. The final rate compared favorably to uninhibited control, since the large dilution resulted in noninhibitory fluoride concentrations. A second experiment (inset) shows much faster reactivation when assayed with 2.5 mM urea. (C) Observed rates for dissociation of the urease−fluoride complex (k_{obs}) were determined (as in panel B, above) for a range of urea concentrations. The line represents the best fit of the data to $k_{obs} = k_{off}\{K_s/(K_s + [urea])\}$, yielding $k_{off} = 0.013\ s^{-1}$ and $K_{s(urea)} = 1.8$ mM.

Scheme 1

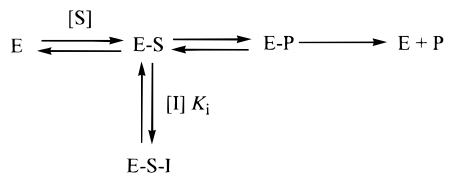

of inhibition is typically observed with multisubstrate enzymes; however, uncompetitive inhibitors could reasonably interact with a hydrolytic enzyme at a site normally occupied by the catalytic water. (2) Parallel double-reciprocal plots also may arise for inhibitors that bind to a form of the enzyme (E*) generated from the active enzyme species (E) during catalysis, as illustrated in Scheme 2 (*26*). According to this underappreciated model, the two enzyme forms are in

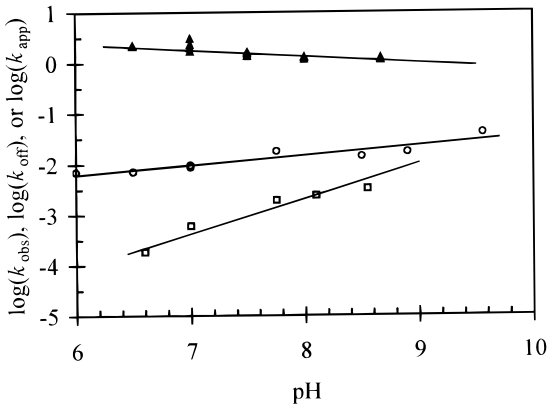

FIGURE 6: pH dependence of k_{app} for fluoride binding and k_{off} or k_{obs} for fluoride dissociation. The second-order rate of fluoride binding (k_{app}, ▲) was measured at the indicated pH values, as described under Experimental Procedures and in Figure 4B. Reactivation of inhibited complex was measured in the absence of urea (○, with k_{off} as obtained in Figure 5A) or in the presence of substrate (□, with k_{obs} as in Figure 5B, 50 mM urea) at the indicated pH values. The log of the rate constants is plotted as a function of pH. Regression analysis gave a slope of 0.19 ± 0.03 (r = 0.86) in the absence of urea and 0.69 ± 0.08 (r = 0.88) in the presence of urea.

Scheme 2

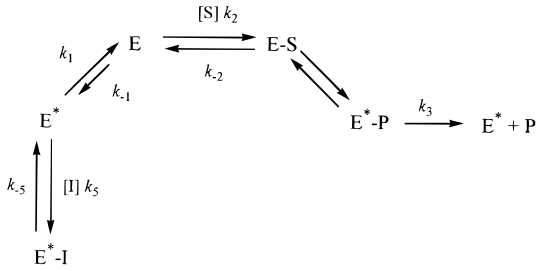

equilibrium in the absence of substrate, but E is highly favored over E* (i.e., $k_1 > k_{-1}$). The steady-state rate equation for this model has been calculated (*26*):

$$v/[E_0] = k_1k_2k_3[S]/\left\{(k_1 + k_3)\,k_2[S] + k_1(k_{-2} + k_3)\left(1 + \frac{k_{-1}}{k_1}\right) + \frac{k_2k_3[I][S]}{K_i} + k_{-1}(k_{-2} + k_3)\,\frac{[I]}{K_i}\right\}$$

where $K_i = k_{-5}/k_5$. In its reciprocal form, this equation rearranges to

$$\frac{[E_0]}{v} = \frac{k_1 + k_3\left(1 + \dfrac{[I]}{K_i}\right)}{k_1k_3} + \frac{(k_{-2} + k_3)\left(1 + \dfrac{k_{-1}}{k_1} + \dfrac{[I]k_{-1}}{K_ik_1}\right)}{k_2k_3[S]}$$

Double-reciprocal plots will show parallel lines when $[I]k_{-1}/(k_1K_i) < 1$ or when $k_{-1}/k_1 \ll 1$.

To distinguish whether urease interaction with fluoride is best modeled by Scheme 1 for classical uncompetitive inhibition or Scheme 2 involving a two-state model for the enzyme (or by another scheme), it is necessary to consider results from pre-steady-state kinetic analyses.

Pre-Steady-State Kinetics for Urease Inhibition by Fluoride. As illustrated in Figure 2, fluoride inhibits a portion of urease activity in the absence of urea but is a far more potent

Scheme 3

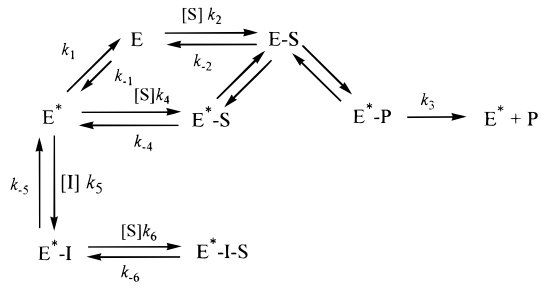

inhibitor in the presence of substrate. Fluoride binding in the absence of substrate is inconsistent with the model shown in Scheme 1 but can be accommodated by that in Scheme 2. In the absence of substrate, the low equilibrium concentration of E* results in only a small portion of enzyme being capable of binding fluoride. Equilibrium is not established rapidly (in <20 s) but requires several minutes (>90% complete in 5 min), allowing a rough estimate of the binding rate of 0.2 $s^{-1} \geq k_{-1} \geq 0.01\ s^{-1}$.

The rate of fluoride binding and the rate of enzyme−fluoride dissociation were both shown to be inhibited by substrate (Figures 4 and 5). This behavior again is inconsistent with classical uncompetitive inhibition (Scheme 1), where the association rate should be enhanced by substrate and the dissociation rate should be substrate-independent. However, substrate inhibition of fluoride binding and dissociation is also inconsistent with the model shown in Scheme 2. To accommodate these results the latter model was modified as shown in Scheme 3. This model includes a complex between urea and the E* form of the enzyme, as well as the ternary complex formed by urea binding to E*·I. Urea inhibition of the apparent fluoride binding rate (Figure 4B) may occur because substrate decreases the concentration of E* (forming E*·S and E·S). Likewise, urea may inhibit the dissociation of fluoride (Figure 5) by stabilizing the ternary complex (E*·I·S). Significantly, the ternary complex described here is distinct in its order of formation from the enzyme−substrate-inhibitor complex associated with classic uncompetitive inhibition. Structural similarity between E, E*, and E*·I is suggested by the finding that the K_m of urea for uninhibited enzyme (2.5 mM, *27*) is similar to the K_s of urea for inhibition of fluoride binding (~10 mM, Figure 4B, involving k_{-4}/k_4) and for inhibition of fluoride dissociation (~2 mM, Figure 5C, involving k_{-6}/k_6). Whereas the E*·I·S species would be catalytically inactive, we expect that the E*·S state may transform to the E·S state since we observe no substrate inhibition for this enzyme.

pH Dependence on K_i, k_{app}, and k_{obs}. Since the equilibrium binding constant, K_i, is the ratio of two microscopic rate constants ($K_i = k_{-5}/k_5$, Scheme 3), the dramatic pH effects on this value (Figure 3B) could be explained by either of two distinct processes: pH-dependent binding or pH-dependent dissociation. In the first case, tighter binding at low pH is caused by an increased rate of *association* upon protonation of either the inhibitor (where the actual inhibitor is HF) or the protein. In the latter case, an increased rate of *dissociation* at elevated pH is responsible for the reduced affinity. Since the association rate appears to be nearly pH-independent (Figure 6), the protonation state must be associated with fluoride *dissociation*, thus eliminating HF

Chart 1

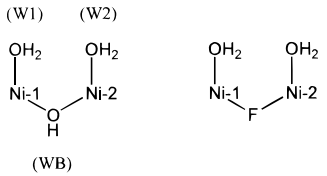

as the actual inhibitor. This was confirmed in Figure 6, where the reactivation rate (measured in the presence of urea) showed strong pH dependence. No inflection was seen in the dissociation rate as a function of pH (from 6.0 < pH < 8.5); therefore the pK_a affecting dissociation must lie outside this range. Two cases would be consistent with such behavior: (1) fluoride dissociation is enhanced upon deprotonation of some group with pK_a > 8.5 or (2) fluoride dissociation is inhibited by protonating some group with pK_a < 6. Currently, we have no experimental data to distinguish between these two cases.

Relationship to Jack Bean Urease Fluoride Inhibition Results. Some of our fluoride inhibition data for *K. aerogenes* urease are consistent with the results reported earlier by Dixon et al. (*12*, *28*) for the jack bean enzyme; however, our interpretations differ considerably from the prior work and we have characterized selected aspects of the inhibition in much greater detail. The investigators working with plant urease emphasized the interaction of fluoride with enzyme in the absence of substrate and described the presence of competitive inhibition with a K_i of about 1 mM at pH 7 (*12*) or 7 μM at pH 5.2 (*28*). Those authors also noted a time-dependence of fluoride inhibition and used steady-state rate data to generate a double-reciprocal plot that consisted of a series of parallel lines (*12*). Although the authors did not use the term "uncompetitive inhibition", they suggested the formation of a urease−substrate−fluoride complex or a urease−carbamato (product)−fluoride complex. Our data obtained with the microbial enzyme have many features that are similar to the published jack bean urease inhibition results, but we interpret our data in terms of the model shown in Scheme 3 that emphasizes formation of E*·F as the initial inhibited species.

Mechanistic Implications Based on the Urease Structure. The crystal structures of urease from *K. aerogenes* and *B. pasteurii* (*1*, *7*−*9*) allow us to speculate on the structural basis of fluoride inhibition, the identity of the E* state, and the pH dependence of fluoride dissociation. Fluoride almost certainly binds to the urease metallocenter with displacement of a water molecule. Three water molecules associated with the metallocenter (W1, W2, and WB) must be considered as possible fluoride binding sites, with our favored binding position shown in Chart 1.

W1, terminally coordinated to Ni-1, cannot be the site of fluoride binding on the basis of our evidence that substrate binds to the E*·F state of the enzyme. Both current urease mechanisms (*1*, *7*) suggest that the urea carbonyl oxygen displaces W1 to bind to Ni-1, with additional stabilization provided by a hydrogen bond from His 219. Structures of acetohydroxamic acid- and phosphorodiamidate-bound forms of the enzyme (*7*, *9*) are also consistent with this mode of urea binding; the oxygen atoms of the substrate analogues coordinate at the W1 position.

On the basis of accessibility arguments, we suggest that W2 is also unlikely to be the site of fluoride binding. According to the model shown in Scheme 3, only a small proportion of resting-state enzyme is capable of binding fluoride to form inhibited enzyme, indicating either that the active site is inaccessible to the inhibitor or that the bound solvent molecule displaced by fluoride is predominantly deprotonated and thus unreactive. Because the metallocenter must be accessible to urea, we favor the second interpretation. Terminally coordinated water such as W2 likely possesses a pK_a of 9−10 (*29*); thus, W2 would be in the protonated state at neutral pH. If this were the site of fluoride inhibition, the enzyme should be nearly completely inhibited under normal pH conditions; however, we have shown this does not occur. A further argument against W2 as the fluoride-binding site is based on the assumption that diamidophosphate-inhibited *B. pasteurii* urease (*7*), where the inhibitor oxygen coordinates to Ni-1 and an amide coordinates to Ni-2, mimics the substrate-bound structure. Since we have shown that urea binds to the fluoride-inhibited enzyme, neither W1 nor W2 can participate in fluoride binding.

Our favored hypothesis is that fluoride binds to the WB site that bridges the two Ni at the active site (Chart 1). This solvent molecule is associated with two pK_a values and three protonation states: the fully protonated species, hydroxide, and dianion. On the basis of studies of a dinuclear nickel model complex, WB may reasonably possess pK_a values of about 4.4 and 8.5 (*30*). If fluoride binding requires dissociation of bridging water, only a small proportion of the enzyme will be reactive for fluoride exchange at neutral pH; little fluoride binding would be expected, as we observe. Following turnover, however, the bridging water site may be vacant or may have a weakly bound, fully protonated water molecule that could be displaced by fluoride. Thus, the equilibrium amount of fluoride-bound urease will increase, as is observed. Once fluoride binds, the protein structure could easily accommodate binding of substrate, consistent with our data. The resulting enzyme−fluoride−urea complex resembles that formed by a classic uncompetitive mechanism but differing in the order of its formation. Steric constraints dictate that fluoride binds before urea. Also consistent with fluoride binding to the WB site, β-mercaptoethanol binds to the bridging position of the urease metallocenter according to X-ray absorption, variable-temperature magnetic circular dichroism, and crystallographic studies (*31*−*33*), and UV−visible spectrophotometric studies of jack bean urease show competition between fluoride and β-mercaptoethanol for binding (*12*). Furthermore, fluoride is known to bind at a bridging position of several binuclear metal model complexes (*34*, *35*) and has been suggested to insert into the bridging position of the dinuclear core in manganese catalase (*36*). Finally, fluoride is suggested to occupy the di-iron bridging site in purple acid phosphatase from porcine uterus (uteroferrin) on the basis of X-ray absorption and resonance Raman spectroscopic analyses (*19*); however, the opposite conclusion was reached by other investigators for a closely related enzyme (*14*).

The observed pH dependence of fluoride dissociation in the presence of urea can also be interpreted in terms of the urease structure and the fluoride-binding mode shown in Chart 1. Deprotonation of W2 (if still present when substrate is bound) could lead to a decreased affinity for the bridging

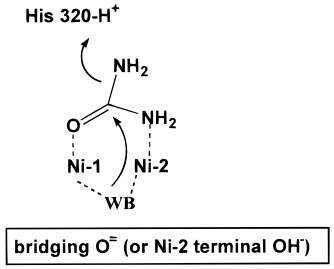

FIGURE 7: Alternative proposal for the urease mechanism. On the basis of results related to urease inhibition by fluoride, we propose that WB is the nucleophilic water molecule. The results of mutational studies (*37* and unpublished results) provide strong support for His 320 serving as the general acid. To explain the observed pH dependence of catalysis, we suggest that the nucleophile has pK_a ~ 9 and the general acid possesses pK_a ~ 6.5, compatible with a reversed protonation mechanism. The pK_a of 9 associated with WB is consistent either with the oxodianion bridging species or the hydroxy species that is terminally coordinated to Ni-2 (formed upon substrate binding). Urea is shown in a chelate binding mode, analogous to the O and N coordination to the two metals seen in diamidophosphate-inhibited urease (*7*), but we cannot exclude the possibility that only the carbonyl oxygen is bound to Ni-1 and that Ni-2 may retain coordination to W2.

ligand and restoration of activity. However, the pH-dependent dissociation is not observed in the absence of substrate. Alternatively, protonation of His 320 or some other protein side chain may decrease the rate of dissociation in the presence of urea. For example, the closed flap configuration that is likely to exist for the substrate- and fluoride-bound enzyme may be stabilized at low pH, thus inhibiting fluoride release. Higher pH may allow the protein flap to open, substrate to be released, and inhibitor to dissociate, in agreement with the data.

Our proposal that fluoride inhibits urease by replacing WB leads to an important insight into the mechanism of catalysis. The mechanism shown in Figure 1A does not require loss of WB upon product dissociation, providing no opportunity for binding of fluoride. In contrast, the nucleophilic nature of WB in the mechanism of Figure 1B ensures loss of this group upon product dissociation, allowing fluoride to bind. Fluoride replacement of the catalytic nucleophile provides a simple explanation for why the enzyme−fluoride complex is inactive. However, the mechanism of Figure 1B does not explain the essential role of His 320 as demonstrated by mutational analysis (*37*; manuscript in preparation). Thus, we propose a revised urease mechanism (Figure 7) that invokes WB as the attacking nucleophile (as in Figure 1B) and His 320 as the general acid (as in Figure 1A). For this reverse protonation mechanism, we suggest that the nucleophile possesses a pK_a near 9 and the general acid has a pK_a of ~6.5. Model studies of a dinuclear nickel complex are consistent with a bridging water undergoing successive deprotonations at pH 4.4 and 8.5 (*30*), in agreement with the oxodianion serving as the nucleophile. Alternatively, the interaction between Ni-1 and WB may weaken upon substrate binding so that the pK_a ~9 is associated with the WB hydroxide terminally coordinated to Ni-2. Both of these possibilities result in an increase in nucleophilicity compared to that for hydroxide bridging two metals.

Relevance of the Fluoride Inhibition Model to Other Metallohydrolases. The models illustrated in Schemes 2 and 3 may also apply to cases of apparent uncompetitive inhibition by fluoride reported for other dinuclear hydrolases. For example, fluoride is a slow-binding inhibitor of bovine spleen purple acid phosphatase (a $Fe^{3+}Fe^{2+}$ or $Fe^{3+}Zn^{2+}$ enzyme) that, on the basis of careful spectroscopic characterization of an enzyme−phosphate (product)−fluoride complex, was suggested to form an enzyme−substrate−fluoride inhibited complex (*14*). Fluoride was shown to be a significantly better inhibitor at lower pH for this enzyme. As already mentioned, spectroscopic studies of the related enzyme uteroferrin led to the proposal that fluoride replaces the bridging hydroxide of this enzyme (*19*). Rat liver inorganic pyrophosphatase (a zinc-dependent enzyme) is inhibited by fluoride with biphasic kinetics, resulting in a rapid initial decrease in activity followed by a slow inactivation during catalysis (*15*). The authors proposed a model in which fluoride bound to the enzyme−substrate complex and this species subsequently underwent a slow isomerization step to form a more inhibited state. Limited pH-dependence studies of that enzyme indicated that inhibition was more pronounced at lower pH values, and the authors suggested that HF is the actual inhibiting species. Aminopeptidases from both *Aeromonas proteolytica* (*16*) and *Streptomyces griseus* (*17*) are inhibited by fluoride by apparent uncompetitive mechanisms, and in both cases the inhibition is pH-dependent with increased inhibition occurring at lower pH. Recent studies of the *A. proteolytica* enzyme showed no evidence for time dependence in the fluoride inhibition (Rick Holz, personal communication). In each of the above examples, the observed results could also be interpreted in terms of inhibitor interaction with an altered E* enzyme form generated during catalysis.

In conclusion, we suggest that Scheme 2 and its derivatives should be included in considerations of apparent uncompetitive inhibition of metallohydrolases by anions. Steady-state kinetic data that exhibit parallel lines in double-reciprocal plots do not conclusively demonstrate the existence of an enzyme−substrate−inhibitor species arising from classic uncompetitive inhibition as commonly invoked.

ACKNOWLEDGMENT

We thank Andy Karplus, Matt Ryle, and Rick Holz for constructive comments.

REFERENCES

1. Karplus, P. A., Pearson, M. A., and Hausinger, R. P. (1997) *Acc. Chem. Res. 30*, 330−337.
2. Mobley, H. L. T., Island, M. D., and Hausinger, R. P. (1995) *Microbiol. Rev. 59*, 451−480.
3. Mulvaney, R. L., and Bremner, J. M. (1981) in *Soil Biochemistry* (Paul, E. A., and Ladd, J. N., Eds.) Vol. 5, pp 153−196, Marcel Dekker, Inc., New York.
4. Zonia, L. E., Stebbins, N. E., and Polacco, J. C. (1995) *Plant Physiol. 107*, 1097−1103.
5. Sumner, J. B. (1926) *J. Biol. Chem. 69*, 435−441.
6. Dixon, N. E., Gazzola, C., Blakeley, R. L., and Zerner, B. (1975) *J. Am. Chem. Soc. 97*, 4131−4133.
7. Benini, S., Rypniewski, W. R., Wilson, K. S., Miletti, S., Ciurli, S., and Mangani, S. (1999) *Structure 7*, 205−216.
8. Jabri, E., Carr, M. B., Hausinger, R. P., and Karplus, P. A. (1995) *Science 268*, 998−1004.
9. Pearson, M. A., Michel, L. O., Hausinger, R. P., and Karplus, P. A. (1997) *Biochemistry 36*, 8164−8172.
10. Pearson, R. M., and Smith, J. A. B. (1943) *Biochem. J. 37*, 148−153.

11. Takishima, K., Mamiya, G., and Hata, M. (1983) in *Frontiers in Biochemical and Biophysical Studies of Proteins and Membranes* (Liu, T.-Y., Skakibara, S., Schechter, A. N., Yagi, K., Yajima, H., and Yasunobu, K. T., Eds.) pp 193−201, Elsevier, New York.
12. Dixon, N. E., Blakeley, R. L., and Zerner, B. (1980) *Can. J. Biochem. 58*, 481−488.
13. Saboury, A. A., and Moosavi-Movahedi, A. A. (1997) *J. Enzyme Inhib. 12*, 273−279.
14. Pinkse, M. W. H., Merkx, M., and Averill, B. A. (1999) *Biochemistry 38*, 9926−9936.
15. Baykov, A. A., Alexandrov, A. P., and Smirnova, I. N. (1992) *Arch. Biochem. Biophys. 294*, 238−243.
16. Chen, G., Edwards, T., D'souza, V. M., and Holz, R. C. (1997) *Biochemistry 36*, 4278−4286.
17. Harris, M. N., and Ming, L. J. (1999) *FEBS Lett. 455*, 321−324.
18. Pocker, Y., and Deits, T. L. (1982) *J. Am. Chem. Soc. 104*, 2424−2434.
19. Wang, X., Ho, R. Y. N., Whiting, A. K., and Que, L., Jr. (1999) *J. Am. Chem. Soc. 121*, 9235−9236.
20. Todd, M. J., and Hausinger, R. P. (1989) *J. Biol. Chem. 264*, 15835−15842.
21. Mulrooney, S. B., Pankratz, H. S., and Hausinger, R. P. (1989) *J. Gen. Microbiol. 135*, 1769−1776.
22. Weatherburn, M. W. (1967) *Anal. Chem. 39*, 971−974.
23. Lowry, O. H., Rosebrough, N. J., Farr, A. J., and Randall, R. J. (1951) *J. Biol. Chem. 193*, 265−275.
24. Chabre, M. (1990) *Trends Biochem. Sci. 15*, 6−10.
25. Segel, H. I. (1975) *Enzyme Kinetics*, John Wiley & Sons, New York.
26. Cennamo, C. (1968) *J. Theor. Biol. 21*, 260−277.
27. Todd, M. J., and Hausinger, R. P. (1987) *J. Biol. Chem. 262*, 5963−5967.
28. Dixon, N. E., Riddles, P. W., Gazzola, C., Blakeley, R. L., and Zerner, B. (1980) *Can. J. Biochem. 58*, 1335−1344.
29. Bertini, I., and Luchinat, C. (1994) in *Bioinorganic Chemistry* (Bertini, I., Gray, H. B., Lippard, S. J., and Valentine, J. S., Eds.) pp 37−106, University Science Books, Mill Valley, CA.
30. Barrios, A. M, and Lippard, S. J. (1999) *J. Am. Chem. Soc. 121*, 11751−11757.
31. Wang, S., Lee, M. H., Hausinger, R. P., Clark, P. A., Wilcox, D. E., and Scott, R. A. (1994) *Inorg. Chem. 33*, 1589−1593.
32. Finnegan, M. G., Kowal, A. T., Werth, M. T., Clark, P. A., Wilcox, D. E., and Johnson, M. K. (1991) *J. Am. Chem. Soc. 113*, 40300-4032.
33. Benini, S., Rypniewski, W. R., Wilson, K. S., Ciurli, S., and Mangani, S. (1998) *J. Biol. Inorg. Chem. 3*, 268−273.
34. Jacobson, R. R., Tyekár, Z., Karlin, K. D., and Zubieta, J. (1991) *Inorg. Chem. 30*, 2035−2040.
35. Lee, S. C., and Holm, R. H. (1993) *Inorg. Chem. 32*, 4745−4753.
36. Meier, A. E., Whittaker, M. M., and Whittaker, J. W. (1996) *Biochemistry 35*, 348−360.
37. Park, I.-S., and Hausinger, R. P. (1993) *Protein Sci. 2*, 1034−1041.

BI992287M